Cullin-associated and neddylation-dissociated 1 protein (CAND1) governs cardiac hypertrophy and heart failure partially through regulating calcineurin degradation

Zhenwei Pan (panzw@ems.hrbmu.edu.cn)
Harbin Medical University https://orcid.org/0000-0002-1011-0954

Xingda Li
Harbin Medical University

Yang Zhang
Harbin Medical University https://orcid.org/0000-0002-6680-3098

Yue Zhao
Harbin Medical University https://orcid.org/0000-0001-7712-6101

Yang Zhou
Harbin Medical University

Qilong Han
Harbin Medical University

Ying Yang
Harbin Medical University

Lingmin Zhang
Harbin Medical University

Ling Shi
Harbin Medical University

Xuexin Jin
Harbin Medical University

Ruixin Zhang
Harbin Medical University

Haiyu Gao
Harbin Medical University

Jiudong Ma
Harbin Medical University

Zheng Li
Harbin Medical University

Gen-Long Xue
Harbin Medical University

Desheng Li
Harbin Medical University
Zhiren Zhang
Third Affiliated Hospital of Harbin Medical University
Yanjie Lu
Harbin Medical University
Baofeng Yang
Harbin Medical University https://orcid.org/0000-0002-0125-1608

Article

Keywords: CAND1, heart failure, calcineurin, ubiquitination, cullin1

Posted Date: March 23rd, 2021

DOI: https://doi.org/10.21203/rs.3.rs-333521/v1

Cullin-associated and neddylation-dissociated 1 protein (CAND1) governs cardiac hypertrophy and heart failure partially through regulating calcineurin degradation

Short title: CAND1 ameliorates cardiac hypertrophy and heart failure

Authors: Xingda Li[1,#], Yang Zhang[1,#], Yue Zhao[1,#], Yang Zhou[1], Qilong Han[1], Ying Yang [1], Lingmin Zhang[1], Ling Shi[1], Xuexin Jin[1], Ruixin Zhang[1], Haiyu Gao[1], Jiudong Ma[1], Zheng Li[1], Genlong Xue[1], Desheng Li[1], Baofeng Yang[1, 2], Zhi-Ren Zhang[3], Yanjie Lu[1, 2], Zhenwei Pan [1, 2*]

Affiliations:[1]Department of Pharmacology, Key Laboratory of Cardiovascular Research, Ministry of Education, College of Pharmacy, Harbin Medical University, Harbin, China, 150086.

[2]Research Unit of Noninfectious Chronic Diseases in Frigid Zone, Chinese Academy of Medical Sciences, China, 2019RU070.

[3]Departments of Cardiology and Clinical Pharmacy, Harbin Medical University Cancer Hospital; Institute of Metabolic Disease, Heilongjiang Academy of Medical Science, Harbin, China.

[*]Corresponding author: Prof. Zhenwei Pan.panzw@ems.hrbmu.edu.cn. Department of Pharmacology, School of Pharmacy, Harbin Medical University, Baojian Road 157, Harbin, Heilongjiang 150081, P. R. China

Fax: 86 451 86675769 or 86667511

Tel: 86 451 86671354

# With equal contributions to the work

Abstract

Cullin-associated and Neddylation-dissociated 1 (CAND1) acts as a coordinator to modulate substrate protein degradation by promoting the formation of specific cullin-based ubiquitin ligase 3 complex in response to the accumulation of specific proteins, which thereby maintains the normal protein homeostasis. However, whether CAND1 titrates the degradation of hypertrophic proteins and manipulates cardiac hypertrophy remains unknown. CAND1 was increased in hypertrophic hearts. CAND1-KO+/- aggravated and CAND1-Tg attenuated cardiac hypertrophy of mice. CAND1 overexpression downregulated the expression of calcineurin, a critical pro-hypertrophic protein. Mechanistically, CAND1 overexpression favored the assembly of Cul1/atrogin1/calcineurin complex and rendered the ubiquitination and degradation of calcineurin. Notably, CAND1 deficiency-induced hypertrophic phenotypes were partially rescued by knockdown of calcineurin, and application of exogenous CAND1 prevented TAC-induced cardiac hypertrophy. Collectively, CAND1 exerts a protective effect against cardiac hypertrophy and heart failure partially by inducing the degradation of calcineurin. CAND1 represents a promising therapeutic target for cardiac hypertrophy and heart failure.

Keywords: CAND1; heart failure; calcineurin; ubiquitination; cullin1

Non-standard Abbreviations and Acronyms

CAND1	Cullin Associated And Neddylation Dissociated 1
UPS	Ubiquitin-proteasome system
CRLs	Cullin-RING family of ubiquitin ligases
FBP	F-box protein
CSN8	COP9-signalosome subunit 8
CSN5	COP9-signalosome subunit 5
NMCMs	Neonatal Mouse Cardiomyocytes
CnA	Calcineurin A
NFATc3	Nuclear factor of activated T cells
Tg	Transgenic
ANF	Atrial natriuretic factor
β-MHC	β-myosin heavy chain
TAC	Transaortic constriction
LVIDd	LV internal dimension at end-diastole
LVIDs	LV internal dimension at systole
EF	Ejection fraction
FS	Fractional shorting
AAV9	Adneo-associated virus-9
Hoxb13	Homeobox protein Hox-B13

Introduction

Cardiac hypertrophy is caused by the disturbance in protein synthesis and degradation in response to the pathological stimuli, which is characterized by the accumulation of hypertrophy-related proteins such as calcineurin, ANF, and β-MHC[1]. Sustained cardiac hypertrophy eventually leads to the development of heart failure and even sudden cardiac death[2].

The ubiquitin-proteasome system (UPS) plays a central role in controlling protein degradation [3]. The UPS mediated protein degradation is deeply involved in the pathogenesis of cardiac hypertrophy and heart failure and represents a promising strategy to treat heart disease[4]. The UPS-mediated protein degradation is a tightly controlled signaling cascade that involves activation of ubiquitin by E1, conjugation of activated ubiquitin by E2 and transfer of ubiquitin chain to substrate by E3 ligase[3]. The cullin-RING family of ubiquitin ligases (CRLs) constitutes the main family of E3 ubiquitin ligases that mediate the ubiquitin-dependent protein degradation in the cell[5, 6]. CRLs exert their E3 ubiquitin ligase activity by forming multi-subunit complexes composed of RING finger proteins, cullin scaffolds(Cul1, 2, 3, 4, 5, 7), adaptor proteins and receptors such as F-box proteins[7, 8]. Generally, the RING finger protein binds to the carboxy-terminal of cullin protein and serves as the site for E2 binding and ubiquitin transfer activity. The adaptor protein assembles with the substrate receptor eg. F-box protein and binds to the amino-terminal of cullin protein for further ubiquitin modification[7, 9]. Disruption of the biological process of cullin complex formation leads to the development of cardiac diseases. For instance, inhibition of cullin neddylation, a necessary step for the formation of cullin complex, induces cardiomyopathy, impairs postnatal cardiac development, and increases susceptibility

to catecholamine-induced cardiac dysfunction[10]. Suppression of cullin deneddylation (an essential step for the formation of cullin complex) by cardiac myocyte specific knockout of the photomorphogenic 9 signalosome subunit 8 (CSN8) leads to cardiac hypertrophy and heart failure [11].

Recently, a novel regulator for the formation of cullin complex named substrate receptor exchange factor, Cullin-Associated and Neddylation-Dissociated 1 (CAND1), was discovered. CAND1 acts as an "coordinator" in demand. Different from neddylation and de-neddylation regulation of cullin complex, the special property of CAND1 is that it does not change the intact biological action of each cullin complex, but accelerates the formation of specific cullin complexes in response to the abnormal accumulation of specific substrates, which therefore increases the efficiency for the degradation of redundant proteins and maintains normal protein homeostasis[12, 13]. However, whether CAND1 participates in the regulation of cardiac hypertrophy by promoting the degradation of hypertrophic related proteins remains unknown.

We therefore in this study explored whether CAND1 plays a critical role in stress-induced cardiac hypertrophy and heart failure. We found that CAND1 acts as a novel anti-hypertrophic regulator to improve the impaired cardiac function partially by facilitating the ubiquitination and degradation of calcineurin.

Results

CAND1 expression is upregulated in hearts of DCM patients and hypertrophic mice

To evaluate the possible role of CAND1 in cardiac hypertrophy, we first compared the expression levels of CAND1 in between the left ventricular tissues from patients with

heart failure (HF) and non-HF subjects. The data showed that the protein level of CAND1 was significantly upregulated in HF relative to non-HF hearts, so were the levels of the hypertrophic marker gene β-myosin heavy chain (β-MHC) (Fig. 1A). Similarly, the levels of CAND1 along with β-MHC and atrial natriuretic factor (ANF) were also significantly upregulated in a mouse model of cardiac hypertrophy induced by thoracic aortic constriction (TAC) for 4 or 6 weeks, compared with the sham-operated controls (Fig. 1B). Consistent to the above findings, higher levels of CAND1, ANF, and β-MHC were also detected in primary cultured neonatal mouse cardiomyocytes (NMCMs) stimulated by angiotensin II (Ang II; 1 μM) to induce cardiomyocyte hypertrophy (Fig. 1C). However, there were no significant increases in CAND1 mRNA levels in human HF hearts, TAC mice hearts, or Ang II-stimulated NMCMs (Fig. 1D-F).

CAND1 plays a critical role in the development of pressure overload-induced heart failure

To evaluate the function of CAND1, we conducted several sets of experiments. First, we assessed the changes of cardiac function in TAC mice using the loss-of-function approach by generating global CAND1-KO mice (Supplemental Fig. 1A). Since the homozygous littermates were embryonically lethal, the heterozygous littermates were used in the study. Decreased expression of CAND1 in the hearts of CAND1-KO$^{+/-}$ mice was confirmed by Western blot analysis (Supplemental Fig. 1B). The CAND1-KO$^{+/-}$ mice did not affect cardiac morphology and function in normal mice without TAC as compared with age- and sex-matched control animals. However, in TAC mice, CAND1-KO$^{+/-}$ caused severe left ventricular dysfunction, as reflected by marked decreases in left ventricular EF% and FS% relative to the values in wild-type

(WT) TAC mice (Fig. 2A). The hypertrophic phenotypes including gross heart size, ratios of heart weight to body weight (HW/BW) and heart weight to tibia length (HW/TL) were significantly increased in WT mice 6 weeks after TAC, and CAND1-KO$^{+/-}$ exaggerated these deleterious alterations (Fig. 2B). In addition, wheat germ agglutinin (WGA) staining and Masson's staining demonstrate that the magnitude of TAC-induced increases in cell size (Fig. 2C) and cardiac fibrosis (Fig. 2D) was greater in CAND1-KO$^{+/-}$ mice than in WT control counterparts. These hypertrophic phenotypes were accompanied by higher degrees of upregulation of the protein and mRNA levels of ANF and β-MHC in CAND1-KO$^{+/-}$ mice than in WT mice (Fig. 2E, F). More strikingly, the death rate of CAND1-KO$^{+/-}$ mice determined at 6 weeks post-TAC was significantly higher than that of WT TAC mice (70% versus 32%; $P < 0.05$) (Fig. 2G).

We then employed gain-of-function study by generating cardiac-specific transgenic mice for CAND1 overexpression (CAND1-TG) (Supplemental Fig. 2A). As illustrated in Supplemental Fig. 2B, among the three independent lines of CAND1-TG mice, line 1 had the highest level of CAND1 expression (≈1.8-fold higher than negative littermates). Therefore, line 1 CAND1-TG mice and their negative littermates were used for subsequent *in vivo* experiments. Echocardiographic measurements showed that EF and FS were both significantly decreased along with enlarged heart size and the ratios of HW/BW and HW/TL in 6-weeks WT TAC mice compared with the sham group, and these deteriorations were essentially abolished in CAND1-TG mice (Fig. 3A, B), indicating a strong anti-hypertrophic property of CAND1. Meanwhile, TAC-induced increases in the areas of cell size (Fig. 3C) and fibrosis (Fig. 3D), as well as in the expression of cardiac hypertrophic biomarker

genes ANF and β-MHC, in WT mice were abrogated in CAND1-TG mice (Fig. 3E, F).

CAND1 attenuates Ang II-induced cardiomyocyte hypertrophy *in vitro*

We then went on to examine whether the effects of CAND1 in the animal model of cardiac hypertrophy could be reproduced in a cellular model of cardiomyocyte hypertrophy. SiCAND1 effectively knocked down the expression level of CAND1 protein in NMCMs (Supplemental Fig. 3A). While siCAND1 did not affect the cross-sectional area of NMCMs under control conditions, it considerably exacerbated Ang II (1 μM)-induced increases in cell size or cardiomyocyte hypertrophy (Supplemental Fig. 3B). In the meantime, siCAND1 also favored Ang II-induced upregulation of the hypertrophic marker genes (Supplemental Fig. 3C, D).

On the other hand, CAND1 overexpression (Supplemental Fig. 3E) produced effects opposite to CAND1 silencing in NMCMs. CAND1 overexpression mitigated Ang II-induced increases in cell size and ANF and β-MHC expression at both protein and mRNA levels (Supplemental Fig. 3F-H).

CAND1 elicits anti-heart failure effects by inducing degradation of calcineurin

Cardiac hypertrophy can be regulated by multiple hypertrophic related proteins. Calcineurin is one of the well-established pro-hypertrophic molecules. It is increased in cardiomyocytes under pathological stress and promotes cardiac hypertrophy by activating the nuclear translocation of nuclear factor of activated T cells (NFAT) to trigger fetal gene expression[14]. In this study, we found that CAND1 suppressed the calcineurin (CnA)/NFAT pathway. Knockout of CAND1 significantly exacerbated TAC-induced upregulation of CnA and nuclear NFATc3 in the left ventricular tissues (Fig. 4A). Oppositely, CAND1-TG substantially mitigated the TAC-induced

upregulation of CnA and nuclear NFATc3 (Fig. 4B). Consistent with the *in vivo* results, hypertrophic increases in the expression of CnA and nuclear localization of NFATc3 were greatly enhanced by CAND1 knockdown in the presence of Ang II (Fig. 4C). Immunofluorescence staining reproduced the result that CAND1 knockdown magnified the Ang II-induced increase in nuclear translocation of NFATc3 (Fig. 4D). Conversely, forced expression of CAND1 diminished the abnormal upregulation of CnA and nuclear NFATc3 stimulated by Ang II (Fig. 4E, F).

It has been documented that ubiquitination of calcineurin is regulated by Cul1/atrogin1 based SCF complex[15], and CAND1 controls the formation of SCF complex in a substrate-dependent manner[13]. These messages urged us to postulate that CAND1 regulates the ubiquitination, thereby the degradation of calcineurin by controlling the formation of Cul1/atrogin1 complex in cardiomyocytes. To examine this notion, we employed coimmunoprecipitation methods using Cul1 and calcineurin antibodies to examine if CAND1 affects the formation of Cul1/atrogin1 complex under different experimental conditions. The level of atrogin1 coimmunoprecipitated with endogenous Cul1 was higher in the left ventricle tissues of WT TAC mice than that of sham controls, and this TAC-induced formation of the atrogin-1 and Cul1 complex was disrupted in the heterozygous CAND1-KO mice (Fig. 5A). Consistently, the coimmunoprecipitation of Cul1 and atrogin1 with endogenous CnA was also impaired in the hearts of CAND1-KO$^{+/-}$ TAC mice than in WT TAC ones (Fig. 5B). The opposite change was observed in CAND1-TG TAC mice. Overexpression of CAND1 promoted the assembly of Cul1/atrogin1/CnA complex in hypertrophic heart, as reflected by increased level of atrogin1 which was pulled down by Cul1, as well as of Cul1 and atrogin1 by calcineurin (Fig. 5C, D).

196 Next, we assessed whether the difference in Cul1/atrogin1/calcineurin complex
197 formation altered the ubiquitination of calcineurin in TAC model of CAND1-KO$^{+/-}$
198 and TG mice. As depicted in Fig. 5E, the ubiquitination of CnA was decreased
199 whereas the protein level of CnA was increased in CAND1-KO$^{+/-}$ mice compared with
200 WT mice after TAC. In contrast, CAND1 overexpression reciprocally enhanced the
201 ubiquitination and reduced the protein levels of CnA after TAC (Fig. 5F). Similarly,
202 knockdown of CAND1 obviously decreased (Supplemental Fig. 4A), whereas
203 overexpression of CAND1 significantly upregulated the ubiquitination level of CnA
204 in Ang II-treated NRCMs (Supplemental Fig. 4B).
205 As stated earlier, CAND1 controls the binding of CnA to atrogin1 leading to
206 degradation of CnA. We reasoned that disrupting the association of CnA with atrogin1
207 by destructing its binding region should then be able to block the pro-hypertrophic
208 pathway. To achieve this object, we created a truncated construct of CnA by deletion
209 mutation of the region encompassing amino acids 287 to 337 that is known to be the
210 binding domain for atrogin1[15]. The truncated version of CnA (CnA$^{\Delta 287\text{-}337}$) while
211 losing the binding capacity to atrogin1 for degradation should maintain its catalytic
212 activity[15]. Successful delivery of CnA$^{\Delta 287\text{-}337}$ and the intact full-length CnA into
213 NRCMs was verified by enormous increases in their protein levels following
214 transfection of their respective constructs (Fig. 6A). Co-transfection of CnA$^{\Delta 287\text{-}337}$,
215 but not full-length CnA, abrogated the suppressive effects of CAND1 overexpression
216 on Ang II-induced increases in cardiomyocyte size and ANF and β-MHC expression
217 (Fig. 6B-D).
218 **Silence of calcineurin rescues TAC-induced cardiac hypertrophy in CAND1-**
219 **KO$^{+/-}$ mice**

If an increase in CnA protein level indeed mediated the pro-hypertrophic phenotypes observed in CAND1-KO mice, then silence of CnA expression should eradicate the detrimental changes of the hearts in TAC mice. To test this point, we injected the AAV9 viral vector carrying an siRNA (AAV9-siCnA) into WT and CAND1-KO mice to silence the expression of CnA. Knockdown of CnA by AAV9-siCnA was first confirmed by the significant reduction of CnA protein levels in the hearts but not by AAV9-siControl (Supplemental Fig. 5A, B). Strikingly but not surprisingly, AAV9-siCnA essentially rescued the depressed EF and FS in both WT and CAND1-KO TAC mice (Fig. 7A). The TAC-induced increases in the ratios of HW/BW and HW/TL and the mean cross-sectional area were effectively mitigated by AAV9-siCnA (Fig. 7B, C), and so was myocardial fibrosis as reported by Masson's staining (Fig. 7D). The improvement of cardiac structure and function consequent to by AAV9-siCnA administration was accompanied by pronounced decreases in the ANF and β-MHC protein levels (Fig. 7E, F).

Qualitatively, the same results were reproduced in our *in vitro* experiments. As exhibited in Fig. 7G, silence of CAND1 by siRNA (siCAND1) dramatically enhanced Ang II–induced increases of cardiomyocyte size and ANF and β-MHC expression compared with the negative control siRNA (siNC), which was essentially reversed by concomitant knockdown of calcineurin with siCnA (Fig. 7H-J). These data indicated that the antihypertrophic effects of CAND1 is at least in part mediated by calcineurin.

TAC-induced cardiac hypertrophy and heart failure are rescued by exogenous CAND1

Another set of rescuing experiments was conducted using adenovirus-mediated CAND1 overexpression (Ad-CAND1; Fig. 8A). Ad-CAND1 was injected through tail

vein into TAC mice at 2 and 6 weeks following the surgery. CAND1 overexpression was confirmed in the hearts of mice two weeks after injection of Ad-CAND1 (Supplemental Fig. 6A, B). As illustrated in Fig. 8B, Ad-CAND1 eminently alleviated the impairment of cardiac function in 10-weeks TAC mice, as reflected by the effective rescuing of the depressed EF and FS. By comparison, Ad-NC did not produce any appreciable effects on TAC-induced cardiac dysfunction. The enlargement of gross size of hearts and the increases in HW/BW and HW/TL ratios with TAC were markedly attenuated by Ad-CAND1, but not by Ad-NC (Fig. 8C). Similarly, Ad-CAND1 abolished the TAC-induced increases of cardiac cells, fibrosis and ANF and β-MHC levels (Fig. 8D-F). As expected, CnA protein level was also significantly downregulated by Ad-CAND1 (Fig. 8G). These results indicate that the cardiac injuries could be well relieved by CAND1 replacement in pressure overload-induced cardiac hypertrophy and heart failure.

Discussion

Cullin-Associated and Neddylation-Dissociated 1 (CAND1) was initially identified as a critical regulator of the cullin complex thereby of ubiquitination and subsequent degradation of proteins for the appropriate maintenance of intracellular protein homeostasis[12, 13]. In the present study, we uncovered that CAND1 is an anti-hypertrophic protein that improves cardiac function in the setting of cardiac hypertrophy and heart failure. The mechanism is partially mediated by promoting the ubiquitination and degradation of calcineurin via enhancing assembly of Cul1/atrogin1/Calcineurin complex (Supplemental Figure 7).

The ubiquitin-proteasome system (UPS) is known to be responsible for the targeted degradation of proteins regulating the imperative signaling pathways in a

variety of human diseases, including cardiac dysfunction[16]. CRLs comprise the largest family of E3/ubiquitin ligase enzymes that regulate the ubiquitination of various substrate proteins by forming cullin based E3 ligase complexes[17]. The normal function of cullin based E3 ligase complex is indispensable for the maintaining of cardiac homeostasis. Several studies have shown that disruption of the complex significantly affects cardiac development and causes cardiac hypertrophy and heart failure[18]. For instance, inhibition of cullin neddylation blocks the formation of CRL and impairs the development of the heart[19]. Knockout of COP9-signalosome subunit 5 (CSN5) suppresses the deneddylation of cullin and leads to cardiac hypertrophy and heart failure[20, 21]. CAND1 is a master regulator of the formation of diverse CRLs. It interacts with deneddylated cullins to form CRL in response to increased specific substrate proteins, which promotes the exchange of substrate adaptors and therefore substrate proteins to maintain protein homeostasis[12, 13]. CAND1 was found abundantly expressed in the heart and liver, moderately in the brain and skeletal muscle, and only slightly in the spleen and lung of rats[22]. However, to the best of our knowledge, the role of CAND1 in cardiac diseases remains unexplored. In this study, we found that in CAND1-deleted mice, the hearts were more vulnerable to damages in TAC-induced cardiac hypertrophy and heart failure. In contrast, CAND1 overexpression with transgenic mice and adenovirus construct produced prominent protective effects against TAC-induced cardiac damages. These data in conjunction with the increase in the protein level of CAND1 in both HF patients and TAC mice suggest that the upregulation of CAND1 under pathological stress is a compensatory mechanism. CAND1 is involved in the general dynamic regulation of CRLs repertoire by acting as an exchange factor for F-box proteins of CRL1 complexes[13]. The formation of new

CRL complexes is substrate dependent. CAND1 is not a component of the CRL complex, and it acts to facilitate the assembly of CRL complexes when more substrates are available, and the subsequent degradation of the substrates, which therefore increases the efficiency of protein degradation[13]. The substrate specificity of an CRL complex is determined by the FBP (F-box protein, eg. atrogin1) that is recruited to the Cul1 scaffold; it is critical for cells to assemble and activate a CRL containing the specific FBP when its substrates are present[23]. Overexpression of atrogin1 increased the formation of cullin1/atrogin1 complex and promoted the ubiquitylation and degradation of calcineurin, and finally inhibited cardiac hypertrophy both *in vivo* and *in vitro*[15]. Here, we found that overexpression of CAND1 increased the formation of cullin1/atrogin1/calcineurin complex and the ubiquitination and degradation of calcineurin, whereas knockout of CAND1 produced the opposite changes.

The calcineurin/NFAT pathway plays a critical role in the pathogenesis of cardiac hypertrophy, in which the activated calcineurin dephosphorylates NFAT to facilitate the translocation of NFAT into nucleus which in turn transactivates the transcription of pro-hypertrophic genes[24]. Blockade of the β isoform of the calcineurin catalytic A-subunit (CaNAβ) polyproline-dependent anchoring by a competing peptide inhibited concentric hypertrophy[25]. Our data revealed that calcineurin mediated the effects of CAND1 on cardiac hypertrophy with its silence eliciting anti-hypertrophic actions in the presence of CAND1 deficiency. Moreover, overexpression of the truncated calcineurin with null ubiquitination by cullin1/atrogin1 complex, successfully induced hypertrophic phenotypes in cardiomyocytes with CAND1 overexpression, whilst overexpression of full-length calcineurin failed to induce cardiac hypertrophy under

the same conditions. The most reasonable explanation is that CAND1 enhanced the ubiquitination and degradation of full length, but not the truncated calcineurin. Calcineurin can also dephosphorylate homeobox protein Hox-B13 (Hoxb13) to promote its nuclear localization and induce cell cycle arrest[26], which imply that CAND1 may participate in cardiomyocyte proliferation due to its regulation on calcineurin.

However, the calcineurin pathway is just one of the signaling pathways involved in cardiac hypertrophy[27]. CAND1 can act as an adaptor/substrate exchanger to alter the CRLs repertoire and determine the turnover of many substrate proteins[23]. We cannot rule out the possibility that CAND1 might also regulate other cullin complexes that can catalyze multiple hypertrophy-related substrate proteins to exert its antihypertrophic effects. CAND1 is also named TBP-interacting protein 120A (TBIP120A) and can directly regulate gene transcription in the nucleus[28], which implies that the mechanisms of CAND1 on cardiac hypertrophy may also manifest at the transcriptional level. These possibilities merit extensive study to get further insight into the regulatory mechanisms of CAND1 in cardiac hypertrophy.

Notably, our results demonstrated that adenovirus-mediated overexpression of CAND1 effectively prevented TAC-induced cardiac hypertrophy and heart failure, implying the therapeutic potential of CAND1. We therefore speculate that CAND1 as a master regulator to titrate redundant substrate degradation may make it a therapeutic target for cardiac hypertrophy and heart failure. Moreover, the special property of CAND1 that it did not change the basic biological function, but enhance the formation rate of CRLs indicates that it may be an ideal therapeutic target for cardiac hypertrophy and heart failure with less adverse effects.

Materials and Methods

Human cardiac samples

Healthy human cardiac samples were collected from the tissue bank of the Heilongjiang Academy of Medical Sciences (Harbin, China), and diseased samples from patients with heart failure (HF). Demographic characteristics of the human subjects from whom the heart tissues were used are summarized in **Supplemental Table 1**. The use of human cardiac tissues for the present study was approved by the Ethics Committee of the Harbin Medical University (No. HMUIRB20170034). Our study protocols complied with the guidelines that govern the use of human tissues outlined in the Declaration of Helsinki.

Animals

Male C57BL/6 mice (weighing 20~25g) were purchased from the Experimental Animal Center of the Harbin Medical University. The animals were kept under standard housing conditions (temperature 21 ± 1°C and humidity 55%~60%) with free access to food and water. Use of animals and the experimental procedures were approved by the Ethic Committees of Harbin Medical University and conformed to the Guide for the Care and Use of Laboratory Animals published by the US National Institutes of Health (NIH Publication No. 85-23, revised 1996).

Generation of CAND1 knockout mice and transgenic mice

Homologous recombination was used to knockout all exons or functional regions of CAND1 gene. CAND1 knockout mice (CAND1 KO, conventional knockout, C57BL/6J) were generated by Cyagen Biosciences Company (China). The strategy for CAND1 KO generation was shown in supplemental Figure1A. RT-PCR method

was used to clone the mouse CAND1 gene, and the CAND1 gene was inserted downstream of the α-MHC promoter to construct CAND1 transgenic mice (CAND1-Tg). The CAND1 transgenic mice were generated by Cyagen Biosciences Company (China). The strategy for CAND1 Tg generation was shown in supplemental Figure2A. The DNA of mice was isolated from the tails and subjected to PCR analysis to identify mice belonging to which type of gene. CAND1 KO mice were identified by PCR analysis using the forward1# (5'-TGCCCTTCCCATCCTCATACCAG-3'), reverse (5'-GGGAAACACTTGCTGGAGTAGACTG-3') primers and forward2# (5'-CGAAGTCAGGCTTAGGGTAGGGAG-3'). For CAND1-Tg mice, the forward (5′-AGAGCCATAGGCTACGGTGTA-3′) and reverse (5′-CAAGGCATTTGACAGCTAAGTTC -3′) primers were used. Male mice were used in the study.

Mouse models of cardiac hypertrophy by transaortic constriction

Transaortic constriction (TAC) was performed following previously described methods[29]. Mice were randomly divided into sham and TAC groups. In each group, mice were anesthetized by injection of avertin (0.2 g/kg, i.p.) for TAC model. The animal was orally intubated with 20-gauge tube, and ventilated (mouse ventilator, UGO BASILE, Biological Research Apparatus, Italy) at the respiratory rate of 100 breaths/min with a tidal volume of 0.3 mL. The transverse aorta was constricted by a 7-0 silk suture ligature tied firmly against a 27-gauge needle between the carotid

arteries. Then, the needle was promptly removed to yield a constriction of 0.4 mm in diameter. The sham operation was consisted of an identical procedure except for the aorta constriction.

Construction of adenovirus carrying CAND1

The adenovirus vector carrying CAND1 gene (Ad-CAND1) was constructed by Cyagen Biosciences Company (China). Mice were given Ad-CAND1 (1.09×10^{11} viral particles/mL) by intravenous injection through tail vein.

Construction of adeno-associated virus 9 (AAV9) carrying calcineurin siRNA

The adeno-associated virus 9 carrying siRNA for calcineurin (AAV9-siCalcineurin) and its negative control construct AAV9-siNC were constructed by Cyagen Biosciences Company (China). Mice were given AAV9-siCalcineurin or AAV9-siNC (1.04×10^{11} viral particles/mL) by intravenous injection through tail vein. After two weeks, mice were subjected to TAC surgery or sham operation for control. Measurements were made six weeks after TAC.

Echocardiography

Left ventricular (LV) function was assessed by echocardiography with an ultrasound machine Vevo2100 (VisualSonics, Toronto, Ontario, Canada) equipped with a 10-MHz phased-array transducer with the M-mode recordings as described previously[30]. Echocardiographic parameters included LV internal dimension at end-diastole (LVIDd), LV internal dimension at systole (LVIDs), ejection fraction (EF), and fractional shortening (FS). EF expressed as percent changes was determined automatically by the machine and FS was calculated according to the equation: ((LVIDd-LVIDs)/LVIDd) × 100.

Histological analysis

Mouse hearts were collected and fixed in 4% paraformaldehyde for 24 h followed by embedding in paraffin according to standard histological protocols. Next, the tissue was cut into 5 μm-thick cross sections. The slices were stained by hematoxylin-eosin (H&E, Solarbio, Beijing, China) and Masson's trichrome (Solarbio, Beijing, China) to evaluate histopathology and collagen volume, respectively. The myocyte cross-sectional areas were measured via fluorescein isothiocyanate-conjugated WGA (L4895; Sigma, St. Louis, MO, USA) staining. Digital images were taken at ×100 or ×200 magnification of 10 random fields from each sample. Fibrosis areas were analyzed by Image-Pro Plus 3.0 (Zeiss). Cell area was calculated by measuring 100 to 150 cells per slide.

Culture and treatment of neonatal mouse cardiomyocytes (NMCMs)

Cardiomyocytes (CMs) were isolated from C57BL/6 mice (1-2 days) as previously described[31]. Briefly, after dissection, hearts were washed and minced in 0.25% trypsin. Pooled cell suspensions were centrifuged and resuspended in Dulbecco's modified Eagle's medium (DMEM Hyclone, USA) supplemented with 10% fetal bovine serum, 100 U/ml penicillin and 100 μg/ml streptomycin. The suspension was incubated in culture flasks for 90 min, which makes fibroblasts preferentially adhere to the bottom of the culture flasks. Neonatal cardiomyocytes were removed from the culture flasks and the medium was changed. Cell cultures were incubated for 48 h at 37 °C in a humidified atmosphere of 95% oxygen and 5% carbon dioxide before any experimentations. To induce hypertrophy, angiotensin II (Ang II, Sigma A9525) was added to the CMs at a concentration of 1 μM for 48 h.

Cell transfection of plasmids and siRNAs

The mouse CAND1 overexpressing plasmid driven by alpha MHC was construct by Cyagen Biosciences (Guangzhou, China). The plasmid carrying full length calcineurin gene with pIRES2-eGFP/Ppp3ca and pIRES2-eGFP/Ppp3ca truncation (287-337) were purchased from Cyagen Biosciences (Guangzhou, China). The constructs (2-3 μg) were transfected into cells using Lipofectamine 2000 (Invitrogen, GrandIsland, NY, USA) according to the manufacturer's instructions. The siRNAs for CAND1 and calcineurin were commercially synthesized by Ribobio (Guangzhou, Guangdong, China), and the sequences were shown in **Table S2**. These constructs were transfected into cells at a concentration of 50 nM using Lipofectamine 2000.

Immunofluorescence

NMCMs were seeded onto laminin-coated coverslips for 24 hours transfection of siCAND1 or CAND1overexpressing plasmids followed by Ang II stimulation for another 24 hours. Then, the cells were fixed with 4% formaldehyde, permeabilized with 0.1% Triton X-100 in PBS for 45 min, and stained with α-actinin (A7811, Sigma; diluted at 1:300) at 4°C overnight. Next, the cells were incubated with a Daylight 594 goat anti-mouse antibody at room temperature for 1 h. The cells were incubated with DAPI for 10 min before immunofluorescence capture. Immunofluorescence was visualized under a fluorescence microscope (Carl Zeiss, 37081). Quantification of cell surface area was achieved by measuring 30 randomly selected cells from 4 independent experiments, and the averaged values were used for analysis. Cell surface area was measured using Image-Pro Plus 6.0 software.

Nuclear and cytoplasmic extraction

The nuclear and cytoplasmic extracts were separated and prepared by using NE-PER nuclear and cytoplasmic extraction reagents (Thermo Fisher Scientific, New York,

CN). Tissues were cut into small pieces and placed in microcentrifuge tubes. CRE I (cytoplasmic extraction reagent I) was added and the tissues were grinded into homogenate. Then the ice-cold CRE II (cytoplasmic extraction reagent II) was added. After centrifugation, the supernatant (cytoplasmic extract) was immediately transferred to a clean tube and the sediment was suspended with NRE (nuclear extraction reagent). After centrifugation, the supernatant was collected as nuclear extract.

Real-time PCR analysis

Cellular RNA was extracted with TRIzol (Invitrogen, California, USA) according to the manufacturer's instruction. TransScript All-in-One First-Strand cDNA Synthesis SuperMix for PCR (TransGen, Beijing, China) was used to prepare cDNA. Quantitative RT-PCR was performed using TransStart Tip Green qPCR SuperMix (TransGen, Beijing, China). Results were quantified using the $2^{-\Delta\Delta CT}$ method. The primers are listed in **Table S3**.

Western blot analysis

Total proteins (50-70 μg) extracted from primary cardiomyocytes or heart tissues were fractionated by SDS-PAGE (8% polyacrylamide gels) and transferred to nitrocellulose membrane. The membrane was blocked with 5% non-fat milk at room temperature for 90 min. The membrane was then incubated with primary antibodies for CAND1 (1:500 dilution; 8759S, Cell Signaling Technology), Calcineurin (1:1000 dilution, 2614S, Cell Signaling Technology), NPPA (1:500 dilution; 27426-1-AP, Proteintech), nuclear factor of activated T cells (NFATc3) (1:500 dilution; 18222-AP, Proteintech), cullin1 (1:500 dilution; 12895-1-AP, Proteintech), β-MHC (1:5000 dilution; M-8421, Sigma), atrogin1 (1:300 dilution; ab-168372, Abcam), and anti-

rabbit IgG (1:1000; 7074S, Cell Signaling Technology) on a shaking bed at 4°C overnight. Then, the membranes were incubated with secondary antibodies (Jackson Immuno Research, West Grove, PA, USA). Western blot bands were analyzed using Odyssey v1.2 software (LICOR Biosciences, Lincoln, NE, USA) by measuring band density and normalizing to β-actin (anti-β-actin,1:10000 dilution, 66009-1-Ig, Proteintech) or Lamin B (anti-Lamin B, 1:500 dilution, 12987-1-AP, Proteintech).

Immunoprecipitation

Immunoprecipitation was performed with the Protein A/G Magnetic Beads (MCE, HY-K0202) system according to the manufacturer's protocols. Briefly, NRCMs or heart tissue lysates were diluted to a concentration of 2 mg/ml. About 500 μg per sample of protein was used for immunoprecipitation. Protein A/G magnetic beads for immunoprecipitation were conjugated with rabbit-anti-Cullin1 antibody or Calcineurin (8 μg antibody per 500 μg protein) and incubated with heart tissue lysates overnight at 4°C with gentle rotation. Beads were collected using centrifugation at 4°C, 10,000× g for 5 min, and beads were washed with cell lysis buffer containing 1% PMSF, three times. The precipitates were diluted with loading buffer and boiled for 10 min at 100°C and later used for Western blotting analyses to detect potential interacting proteins[15, 32].

Ubiquitination of Calcineurin

Neonatal mouse ventricular myocytes were transfected with plasmids overexpressing CAND1, CAND1 siRNA, or a scramble sequence (negative control) and treated with Ang II and 5 μM MG132 (Aladdin) for 24 h. Twenty-four hours later, the cells were harvested for co-immunoprecipitation. Left ventricular tissue was processed for Co-IP

procedures. Co-immunoprecipitation was performed by using a Pierce Co-Immunoprecipitation Kit (Thermo Fisher) according to the manufacturer's instruction. Ubiquitination level of Calcineurin was determined by Western blotting with anti-ubiquitin antibodies (1:200 dilution; 10201-2-AP, Proteintech)[29].

Statistical analysis

For two-group comparisons, unpaired Student's t test was performed. For multiple group comparisons, significance was determined by using one-way analysis of variance (ANOVA) followed by Bonferroni corrected post hoc t test. The survival rate was analyzed by Chi-square test. $P < 0.05$ was considered statistically significant.

Author contributions

Xingda Li, YZ, YZ, performed experiments, analyzed data, and prepared the manuscript. Yang Zhou, QH, YY, LZ, SL, XJ, RZ, HG, JM, ZL, GZ and DL helped perform experiments and collect data. BY, ZZ and YJL oversaw the project and proofread the manuscript. ZP designed the project, oversaw the experiments and prepared the manuscript.

Sources of funding

This work was supported by National Key R&D Program of China (2017YFC1307404 to Z. P.), National Natural Science Foundation of China (81730012, 81861128022 to B. Y. and 81930009 to Z.Z.81870295 to Z. P.), Funds for Distinguished Young Scholars of Heilongjiang Province (to Z. P.).

Competing interests

The authors declare no competing interests.

Data availability

The data that support the findings of this study and unique materials are available from the corresponding authors upon reasonable request. Source data are provided with this paper. Additional data related to this paper may be requested from the authors.

References

1. Frey N, Olson EN. Cardiac hypertrophy: the good, the bad, and the ugly. Annual review of physiology 65, 45-79 (2003).
2. Burchfield JS, Xie M, Hill JA. Pathological ventricular remodeling: mechanisms: part 1 of 2. Circulation 128, 388-400 (2013).
3. Balaji V, Hoppe T. Regulation of E3 ubiquitin ligases by homotypic and heterotypic assembly. F1000Research 9, (2020).
4. Barac YD, et al. The ubiquitin-proteasome system: A potential therapeutic target for heart failure. J Heart Lung Transplant 36, 708-714 (2017).
5. Lin Z, Murtaza I, Wang K, Jiao J, Gao J, Li PF. miR-23a functions downstream of NFATc3 to regulate cardiac hypertrophy. Proc Natl Acad Sci U S A 106, 12103-12108 (2009).
6. A S, T H, ZQ P. The cullin protein family. Genome biology 12, 220 (2011).
7. BA S, et al. Insights into SCF ubiquitin ligases from the structure of the Skp1-Skp2 complex. Nature 408, 381-386 (2000).
8. D G, M P. Oncogenic aberrations of cullin-dependent ubiquitin ligases. Oncogene 23, 2037-2049 (2004).
9. N Z, et al. Structure of the Cul1-Rbx1-Skp1-F boxSkp2 SCF ubiquitin ligase complex. Nature 416, 703-709 (2002).
10. J Z, et al. Transient inhibition of neddylation at neonatal stage evokes reversible cardiomyopathy and predisposes the heart to isoproterenol-induced heart failure. American journal of physiology Heart and circulatory physiology 316, H1406-H1416 (2019).
11. H S, et al. Perturbation of cullin deneddylation via conditional Csn8 ablation impairs the ubiquitin-proteasome system and causes cardiomyocyte necrosis and dilated cardiomyopathy in mice. Circulation research 108, 40-50 (2011).
12. Liu J, Furukawa M, Matsumoto T, Xiong Y. NEDD8 modification of CUL1 dissociates p120(CAND1), an inhibitor of CUL1-SKP1 binding and SCF ligases. Mol Cell 10, 1511-1518 (2002).
13. Pierce NW, et al. Cand1 promotes assembly of new SCF complexes through dynamic exchange of F box proteins. Cell 153, 206-215 (2013).
14. Wilkins BJ, et al. Calcineurin/NFAT coupling participates in pathological, but not physiological,

cardiac hypertrophy. Circulation research 94, 110-118 (2004).
15. Li HH, et al. Atrogin-1/muscle atrophy F-box inhibits calcineurin-dependent cardiac hypertrophy by participating in an SCF ubiquitin ligase complex. J Clin Invest 114, 1058-1071 (2004).
16. Portbury AL, Ronnebaum SM, Zungu M, Patterson C, Willis MS. Back to your heart: ubiquitin proteasome system-regulated signal transduction. Journal of molecular and cellular cardiology 52, 526-537 (2012).
17. Lydeard JR, Schulman BA, Harper JW. Building and remodelling Cullin-RING E3 ubiquitin ligases. EMBO reports 14, 1050-1061 (2013).
18. Cacciapuoti F. Role of ubiquitin-proteasome system (UPS) in left ventricular hypertrophy (LVH). American journal of cardiovascular disease 4, 1-5 (2014).
19. Wang X, Martin DS. The COP9 signalosome and cullin-RING ligases in the heart. Am J Cardiovasc Dis 5, 1-18 (2015).
20. Kameda K, et al. CSN5/Jab1 inhibits cardiac L-type Ca2+ channel activity through protein-protein interactions. Journal of molecular and cellular cardiology 40, 562-569 (2006).
21. Walweel K, Laver DR. Mechanisms of SR calcium release in healthy and failing human hearts. Biophysical reviews 7, 33-41 (2015).
22. Yogosawa S, et al. Induced expression, localization, and chromosome mapping of a gene for the TBP-interacting protein 120A. Biochemical and biophysical research communications 266, 123-128 (1999).
23. Liu X, Reitsma JM, Mamrosh JL, Zhang Y, Straube R, Deshaies RJ. Cand1-Mediated Adaptive Exchange Mechanism Enables Variation in F-Box Protein Expression. Mol Cell 69, 773-786 e776 (2018).
24. Molkentin JD, et al. A calcineurin-dependent transcriptional pathway for cardiac hypertrophy. Cell 93, 215-228 (1998).
25. Li X, et al. Calcineurin Abeta-Specific Anchoring Confers Isoform-Specific Compartmentation and Function in Pathological Cardiac Myocyte Hypertrophy. Circulation 142, 948-962 (2020).
26. Nguyen NUN, et al. A calcineurin-Hoxb13 axis regulates growth mode of mammalian cardiomyocytes. Nature 582, 271-276 (2020).
27. Nakamura M, Sadoshima J. Mechanisms of physiological and pathological cardiac hypertrophy. Nature reviews Cardiology 15, 387-407 (2018).
28. Kayukawa K, Kitajima Y, Tamura T. TBP-interacting protein TIP120A is a new global transcription activator with bipartite functional domains. Genes to cells : devoted to molecular & cellular mechanisms 6, 165-174 (2001).
29. Cai B, et al. Long Noncoding RNA-DACH1 (Dachshund Homolog 1) Regulates Cardiac Function by Inhibiting SERCA2a (Sarcoplasmic Reticulum Calcium ATPase 2a). Hypertension 74, 833-842 (2019).
30. Pan Z, et al. MicroRNA-101 inhibited postinfarct cardiac fibrosis and improved left ventricular compliance via the FBJ osteosarcoma oncogene/transforming growth factor-beta1 pathway. Circulation 126, 840-850 (2012).
31. Wang J, et al. MicroRNA-24 regulates cardiac fibrosis after myocardial infarction. J Cell Mol Med 16, 2150-2160 (2012).
32. Xie X, et al. The immunoproteasome catalytic beta5i subunit regulates cardiac hypertrophy by

603 targeting the autophagy protein ATG5 for degradation. Science advances 5, eaau0495 (2019).
604
605

606 **Figure Legends**

607 **Figure 1. Upregulation of protein levels of CAND1 in human heart failure**
608 **patients and models of cardiac hypertrophy. (A)** Protein levels of β-MHC (β-
609 myosin heavy chain) and CAND1 in left ventricular tissues of human non-heart
610 failure (HF) subjects and heart failure patients (n = 4). **(B)** Protein levels of ANF, β-
611 MHC, and CAND1 in left ventricular tissues of hypertrophic mice after 4- and 6-
612 weeks sham or TAC operation (n = 6 mice/group). **(C)** Protein levels of ANF, β-MHC,
613 and CAND1 in neonatal mouse cardiomyocytes (NMCMs) treated with either PBS as
614 a control or angiotensin II (Ang II; 1 μM) for 24 and 48 h (n = 6/group). **(D)** The
615 mRNA levels of CAND1 in the human hearts of healthy and heart failure (HF)
616 patients (n=3 hearts/group). **(E)** mRNA levels of CAND1 in the mouse left ventricle
617 tissues at 4 and 6 weeks after sham or TAC operation (n=4-5 mice/group). **(F)** mRNA
618 levels of CAND1 in NRCMs treated with Ang II (1 μM) for 24 and 48 hours
619 (n=9/group). ns indicates no significance. *$P < 0.05$.

620 **Figure 2. CAND1 heterozygous knockout aggravate TAC-induced cardiac**
621 **hypertrophy. (A)** Representative images of M-mode echocardiography on the left
622 ventricle (top) and statistical data of ejection fraction (EF%) and fractional shortening
623 (FS%) (n = 8-10). **(B)** H&E staining of cardiac sections and statistical analysis of
624 HW/BW and HW/TL ratios (n = 8-10). **(C)** Images of wheat germ agglutinin (WGA)
625 staining and mean values of relative myocyte cross-sectional areas (200 cells counted
626 per heart; n = 5). **(D)** Masson's trichrome staining in cardiac sections and percent
627 fibrotic areas (n = 5). **(E)** ANF protein (n = 4) and mRNA (n = 5) levels. **(F)** β-MHC
628 protein (n = 6) and mRNA (n = 5) levels. **(G)** Survival rate in TAC mice with
629 CAND1-KO$^{+/-}$ (n = 19) relative to wild type (WT) TAC mice (n = 17). Data are

presented as mean ± SEM, and n represents the number of animals per group. *$P <$ 0.05 versus WT + Sham; $^{\#}P < 0.05$ versus WT + TAC.

Figure 3. CAND1 overexpression in transgenic mice (CAND1-TG) produces anti-hypertrophic effects. **(A)** Representative images of M-mode echocardiography and statistical analysis of EF and FS (n = 8-10). **(B)** H&E staining of cardiac sections and statistical analysis of HW/BW and HW/TL ratios (n=8-10). **(C)** WGA staining images and statistical results of the relative myocyte cross-sectional area (200 cells counted per heart; n = 5). **(D)** Masson's trichrome staining images and statistical data of percent changes of fibrosis area (n = 5). **(E)** Protein (n = 4) and mRNA (n = 5) levels of ANF. **(F)** Protein (n = 6) and mRNA (n = 5) levels of β-MHC. Data are presented as mean ± SEM, and n represents the number of animals per group. *$P < 0.05$ versus WT + Sham; $^{\#}P < 0.05$ versus WT + TAC.

Figure 4. CAND1 suppressed the calcineurin (CnA)/NFAT pathway. (A) calcineurin (n = 6) and nuclear NFATc3 (n = 6) in TAC mice with or without CAND1 KO. **(B)** Protein levels of calcineurin (n = 6) and nuclear NFATc3 (n = 6) in TAC mice with or without CAND1 TG. **(C)** Protein levels of CnA (n = 6) and nuclear NFAT in cardiomyocytes with siCAND1 (n = 5). NC, negative control. **(D)** Representative immunostaining images (upper) and statistical data (lower) showing that siCAND1 promoted nuclear translocation of NFATc3 (green indicates NFAT; blue represents nuclei). **(E)** Overexpression of CAND1 decreased the protein levels of CnA (n = 6) and nuclear NFATc3 in cardiomyocytes (n = 6). **(F)** Overexpression of CAND1 inhibited nuclear translocation of NFATc3 evaluated by immunostaining (green represents NFATc3; blue indicates nuclei). Data are presented as mean ± SEM, *$P <$

0.05 versus WT, NC + PBS or GFP + PBS; $^{\#}P < 0.05$ versus WT + TAC, NC + Ang II or GFP + Ang II. Lamin B was used as internal control for nuclear NFATc3.

Figure 5. CAND1 induces the ubiquitination and degradation of calcineurin. (A, B) Left ventricular lysate of CAND1-KO$^{+/-}$ TAC mice immunoprecipitated with anti-Cul1 antibody and then immunoblotted atrogin1, or immunoprecipitated with anti-CnA antibody and then immunoblotted atrogin1 and Cul1. The blotted protein was quantified(n = 3). **(C, D)** Left ventricular lysate of CAND1-TG TAC mice immunoprecipitated with anti-Cul1 antibody and then immunoblotted atrogin1, or immunoprecipitated with anti- CnA antibody and then immunoblotted atrogin1 and Cul1. The blotted protein was quantified(n = 3). **(E, F)** Lysates from heart tissues of CAND1-KO$^{+/-}$ TAC or CAND1-TG TAC mice were immunoprecipitated with anti-CnA antibody and blotted with anti-ubiquitin or CnA antibody. Quantification of the relative ubiquitinated CnA level (n = 3) and input. β-actin as an internal control. $^{*}P < 0.05$ versus WT + Sham; $^{\#}P < 0.01$ versus WT + TAC.

Figure 6. Truncated calcineurin (CnA$^{\Delta 287\text{-}337}$), but not full-length CnA, abrogated the suppressive effects of CAND1 overexpression on Ang II-induced cardiomyocyte hypertrophy. (A) Protein levels of calcineurin (CnA) in NMCMs transfected with GFP, CnA (WT) and CnA $^{\Delta 287\text{-}337}$ (n = 7; $^{*}P<0.05$). **(B)** Transfection of CnA (WT) and CnA$^{\Delta 287\text{-}337}$ differentially affected protective effects of CAND1 on Ang II-induced enlargement of cardiomyocytes, as indicated by representative images of double immunostaining (green represents α-actinin for cardiomyocytes; blue indicates DAPI for nuclei). **(C)** Quantification of myocyte surface area plotted from the data shown in (**B**) (30 cells counted per experiment; n = 5; $^{*}P < 0.05$). **(D)** Protein

levels of ANF (n = 5; *$P < 0.05$) and β-MHC (n = 7; *$P < 0.05$) obtained under indicated experimental conditions.

Figure 7. Knockdown of calcineurin improves TAC-induced cardiac dysfunction in CAND1-KO$^{+/-}$ mice. (A) Representative M-mode echocardiography of the hearts and statistical analysis of EF and FS (n = 7-9). **(B)** Heart size by H&E staining and HW/BW and HW/TL ratios calculated (n = 7-9). **(C)** Cardiomyocyte size detected by WGA staining and Quantification of the relative myocyte cross-sectional area (200 cells counted per heart) (n = 5) **(D)** Fibrosis detected by Masson's trichrome staining (n = 5). **(E, F)** The protein levels of ANF (n = 4) and β-MHC (n = 6). **(G)** Knockdown efficiency of the siRNAs for CnA in NMCMs (n = 3; *$P < 0.05$). **(H)** Representative images of α-actinin and DAPI staining. **(I)** Quantification of myocyte surface areas (30 cells counted per experiment; n = 5). **(J)** Protein levels of ANF (n = 5) and β-MHC (n = 7) in NMCMs. Data are presented as mean ± SEM. * $P < 0.05$ between indicated groups.

Figure 8. CAND1 overexpression produces anti-hypertrophic effects in TAC model. (A) Representative of the procedures of Ad-CAND1 administration. **(B)** Representative M-mode echocardiography of the hearts and statistical analysis of EF and FS (n = 8). **(C)** Heart size detected by H&E staining and HW/BW and HW/TL ratios calculated (n = 8). **(D)** Cardiomyocyte size detected by WGA staining and quantification of the relative myocyte cross-sectional area (200 cells counted per heart) (n = 5). **(E)** Cardiac fibrosis detected by Masson's trichrome staining and quantification of fibrotic area (n = 5). **(F, G)** The protein levels of ANF, β-MHC and CnA in the left ventricle (n=4). *$P < 0.05$, versus WT + V-NC; $^{\#}P < 0.5$, versus WT + TAC + V-NC.

Figures

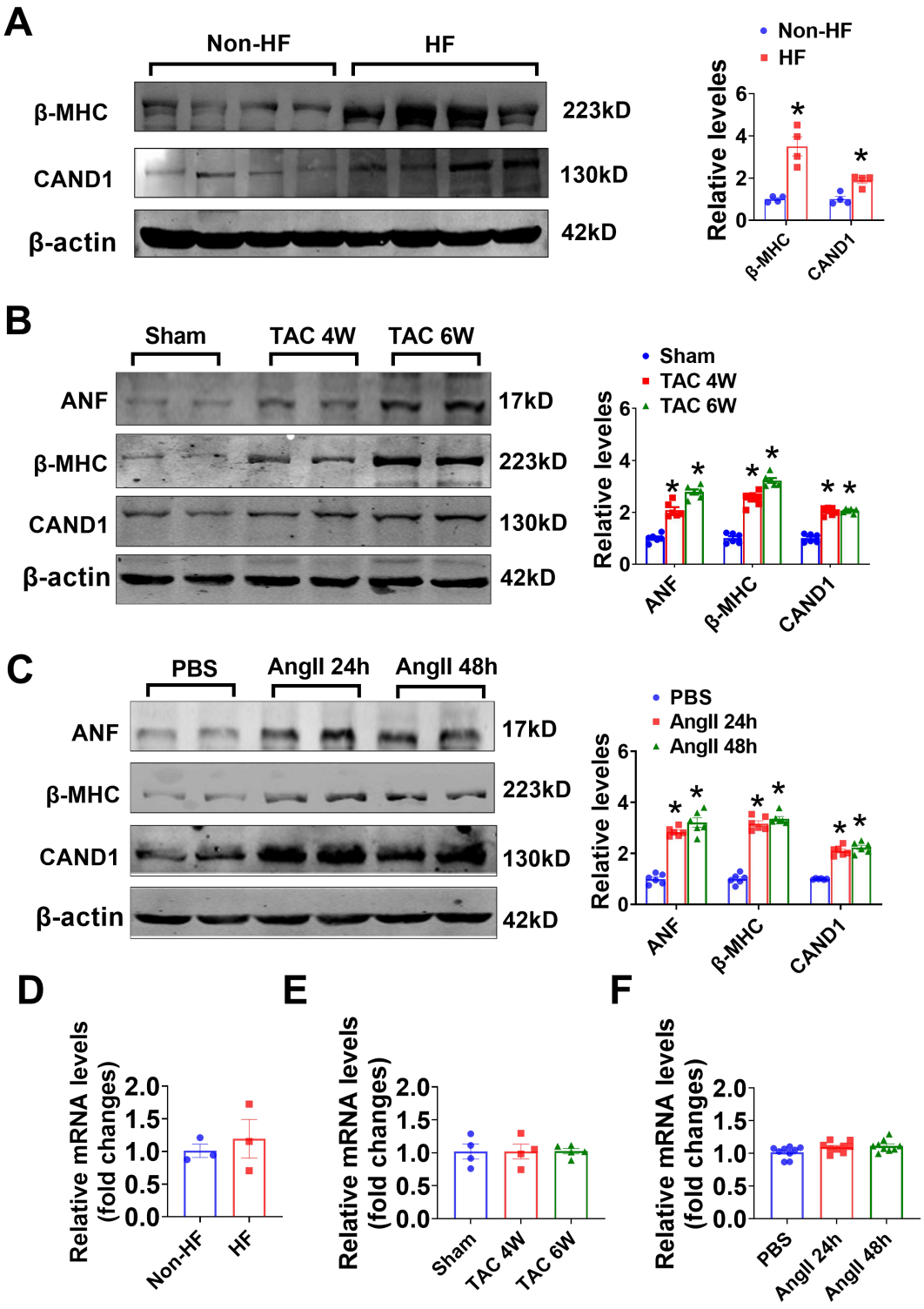

Figure 1

Upregulation of protein levels of CAND1 in human heart failure patients and models of cardiac hypertrophy. (A) Protein levels of β-MHC (β- myosin heavy chain) and CAND1 in left ventricular tissues of human non-heart failure (HF) subjects and heart failure patients (n = 4). (B) Protein levels of ANF, β- MHC,

and CAND1 in left ventricular tissues of hypertrophic mice after 4- and 6- weeks sham or TAC operation (n = 6 mice/group). (C) Protein levels of ANF, β-MHC, and CAND1 in neonatal mouse cardiomyocytes (NMCMs) treated with either PBS as a control or angiotensin II (Ang II; 1 μM) for 24 and 48 h (n = 6/group). (D) The mRNA levels of CAND1 in the human hearts of healthy and heart failure (HF) patients (n=3 hearts/group). (E) mRNA levels of CAND1 in the mouse left ventricle tissues at 4 and 6 weeks after sham or TAC operation (n=4-5 mice/group). (F) mRNA levels of CAND1 in NRCMs treated with Ang II (1 μM) for 24 and 48 hours (n=9/group). ns indicates no significance. *P < 0.05.

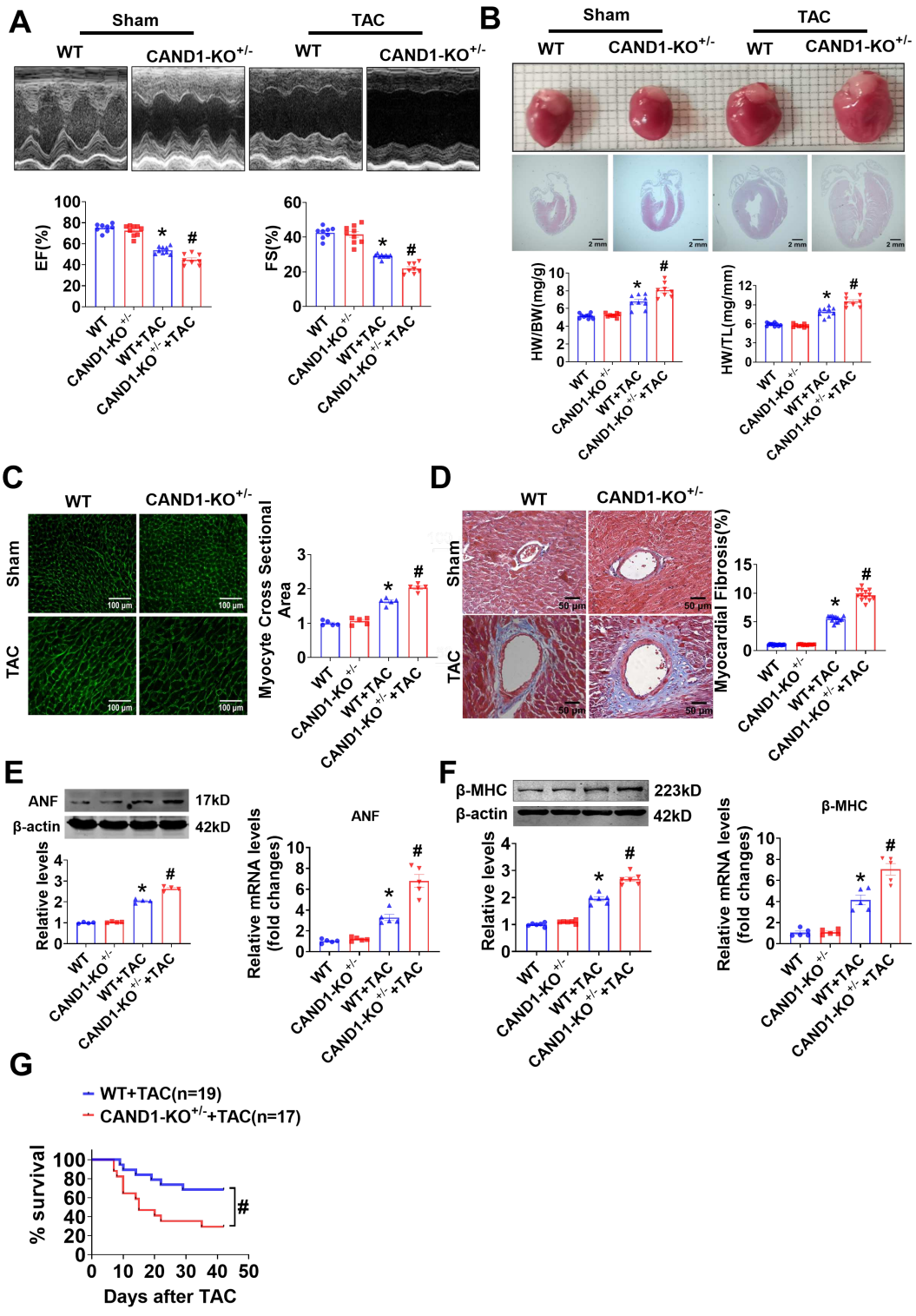

Figure 2

CAND1 heterozygous knockout aggravate TAC-induced cardiac hypertrophy. (A) Representative images of M-mode echocardiography on the left ventricle (top) and statistical data of ejection fraction (EF%) and fractional shortening (FS%) (n = 8-10). (B) H&E staining of cardiac sections and statistical analysis of HW/BW and HW/TL ratios (n = 8-10). (C) Images of wheat germ agglutinin (WGA) staining and mean values of relative myocyte cross-sectional areas (200 cells counted per heart; n = 5). (D) Masson's trichrome staining in cardiac sections and percent fibrotic areas (n = 5). (E) ANF protein (n = 4) and mRNA (n = 5) levels. (F) β-MHC protein (n = 6) and mRNA (n = 5) levels. (G) Survival rate in TAC mice with CAND1-KO+/- (n = 19) relative to wild type (WT) TAC mice (n = 17). Data are presented as mean ± SEM, and n represents the number of animals per group. *P < 0.05 versus WT + Sham; #P < 0.05 versus WT + TAC.

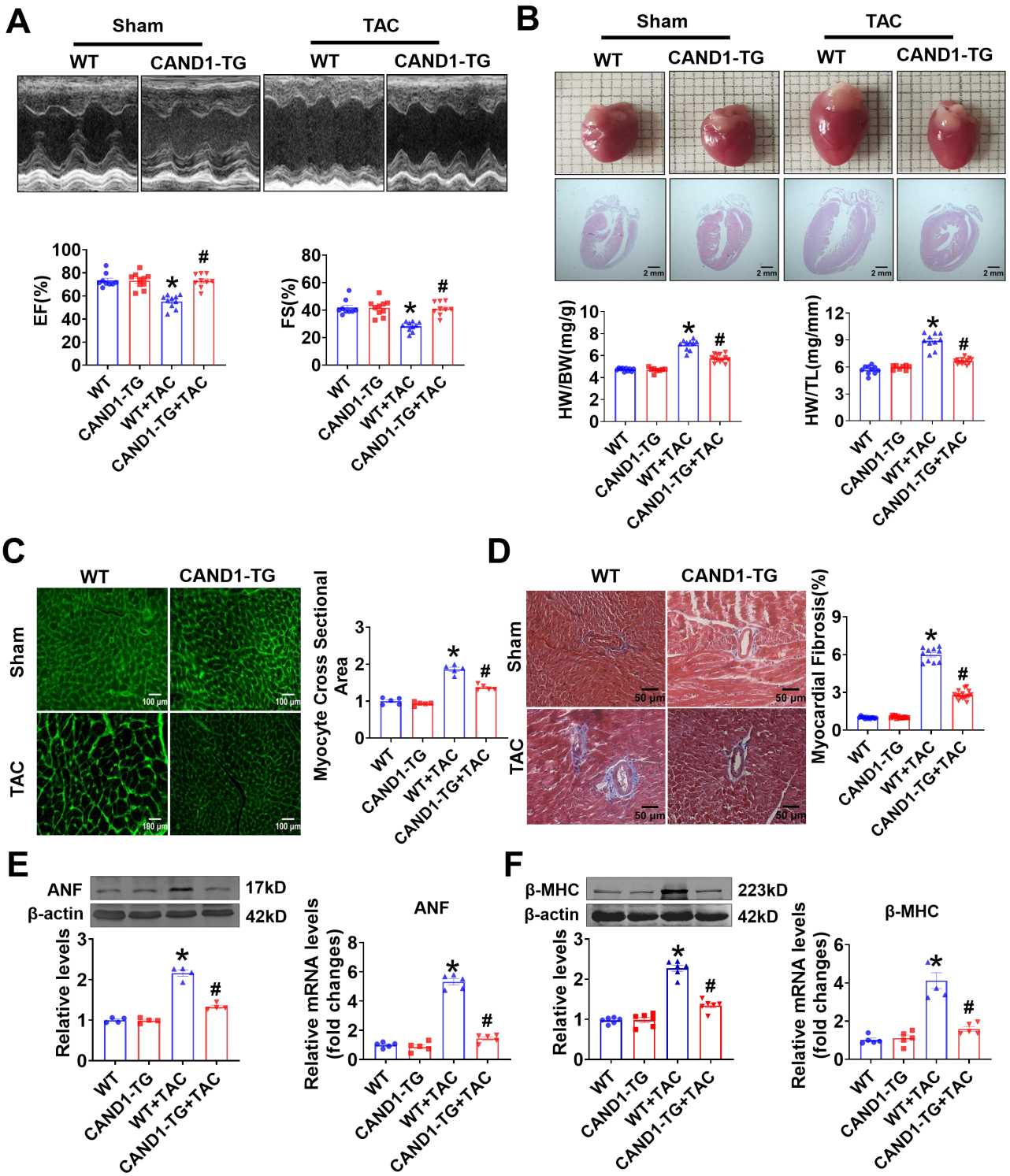

Figure 3

CAND1 overexpression in transgenic mice (CAND1-TG) produces anti- hypertrophic effects. (A) Representative images of M-mode echocardiography and statistical analysis of EF and FS (n = 8-10). (B) H&E staining of cardiac sections and statistical analysis of HW/BW and HW/TL ratios (n=8-10). (C) WGA staining images and statistical results of the relative myocyte cross-sectional area (200 cells counted per heart; n = 5). (D) Masson's trichrome staining images and statistical data of percent changes of fibrosis

area (n = 5). (E) Protein (n = 4) and mRNA (n = 5) levels of ANF. (F) Protein (n = 6) and mRNA (n = 5) levels of β-MHC. Data are presented as mean ± SEM, and n represents the number of animals per group. *P < 0.05 versus WT + Sham; #P < 0.05 versus WT + TAC.

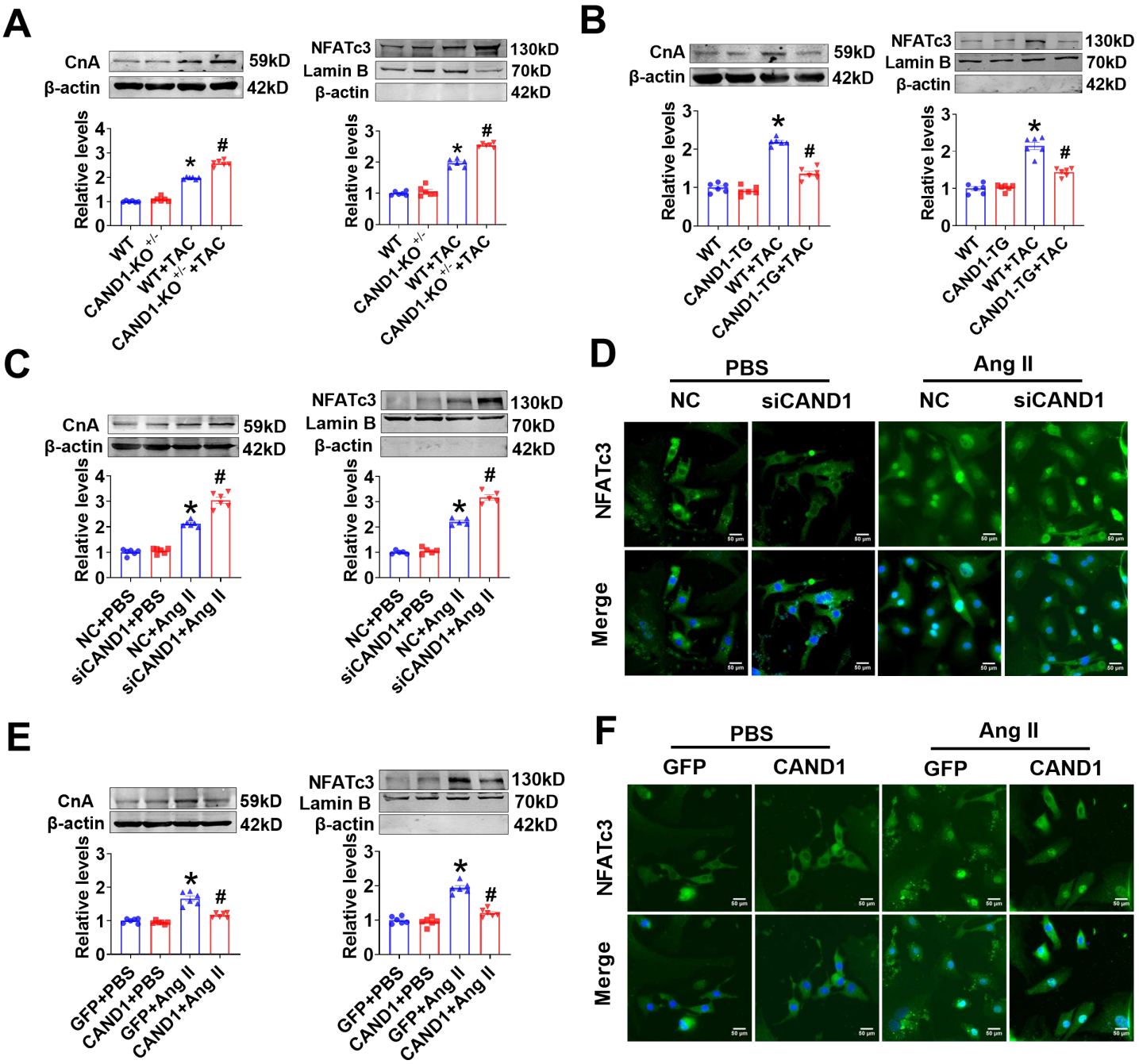

Figure 4

CAND1 suppressed the calcineurin (CnA)/NFAT pathway. (A) calcineurin (n = 6) and nuclear NFATc3 (n = 6) in TAC mice with or without CAND1 KO. (B) Protein levels of calcineurin (n = 6) and nuclear NFATc3 (n = 6) in TAC mice with or without CAND1 TG. (C) Protein levels of CnA (n = 6) and nuclear NFAT in cardiomyocytes with siCAND1 (n = 5). NC, negative control. (D) Representative immunostaining images (upper) and statistical data (lower) showing that siCAND1 promoted nuclear translocation of NFATc3

(green indicates NFAT; blue represents nuclei). (E) Overexpression of CAND1 decreased the protein levels of CnA (n = 6) and nuclear NFATc3 in cardiomyocytes (n = 6). (F) Overexpression of CAND1 inhibited nuclear translocation of NFATc3 evaluated by immunostaining (green represents NFATc3; blue indicates nuclei). Data are presented as mean ± SEM, *P < 0.05 versus WT, NC + PBS or GFP + PBS; #P < 0.05 versus WT + TAC, NC + Ang II or GFP + Ang II. Lamin B was used as internal control for nuclear NFATc3.

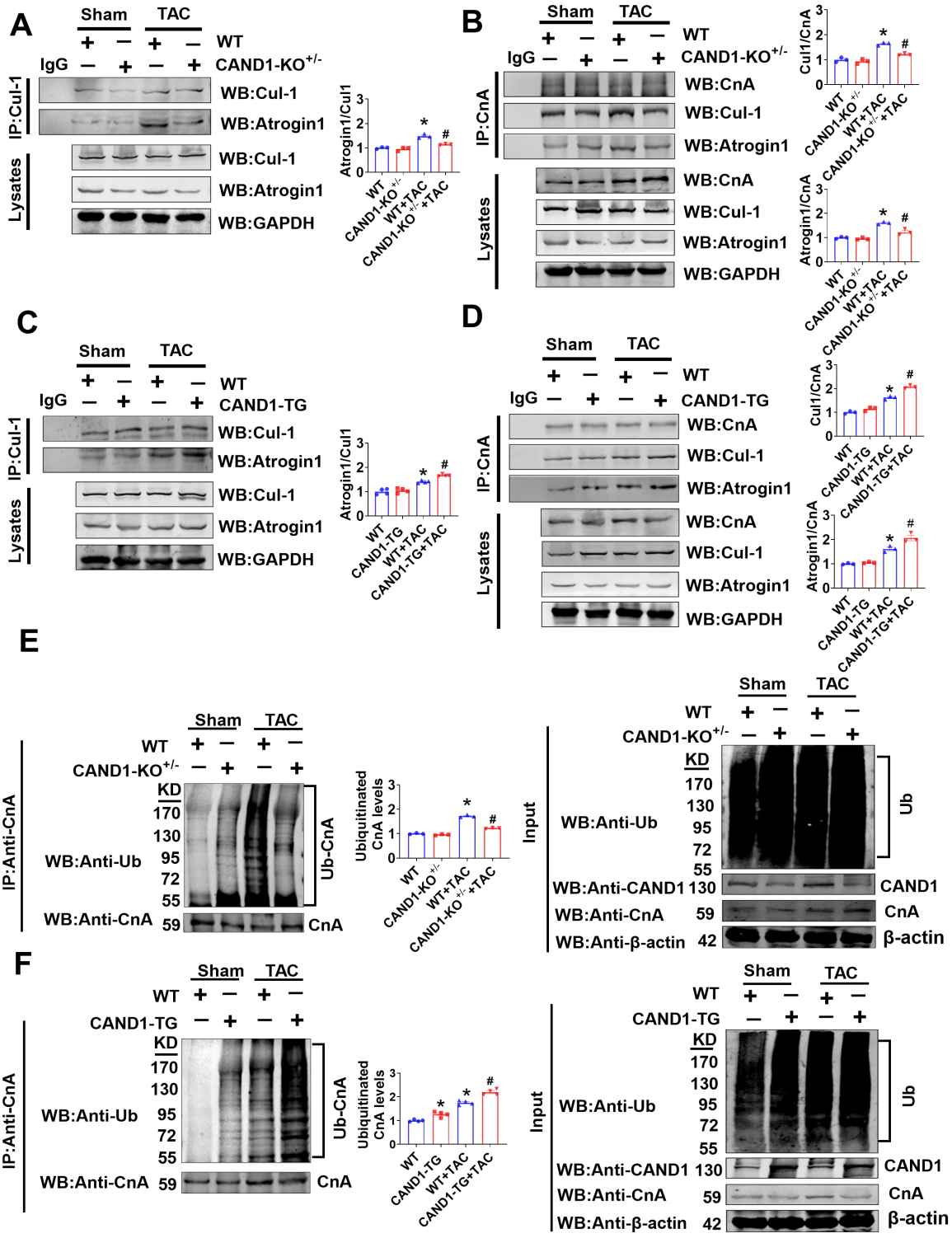

Figure 5

CAND1 induces the ubiquitination and degradation of calcineurin. (A, B) Left ventricular lysate of CAND1-KO+/- TAC mice immunoprecipitated with anti- Cul1 antibody and then immunoblotted atrogin1, or immunoprecipitated with anti- CnA antibody and then immunoblotted atrogin1 and Cul1. The blotted protein was quantified(n = 3). (C, D) Left ventricular lysate of CAND1-TG TAC mice immunoprecipitated with anti-Cul1 antibody and then immunoblotted atrogin1, or immunoprecipitated with anti- CnA antibody and then immunoblotted atrogin1 and Cul1. The blotted protein was quantified(n = 3). (E, F) Lysates from heart tissues of CAND1-KO+/- TAC or CAND1-TG TAC mice were immunoprecipitated with anti- CnA antibody and blotted with anti-ubiquitin or CnA antibody. Quantification of the relative ubiquitinated CnA level (n = 3) and input. β -actin as an internal control. *P < 0.05 versus WT + Sham; #P < 0.01 versus WT + TAC.

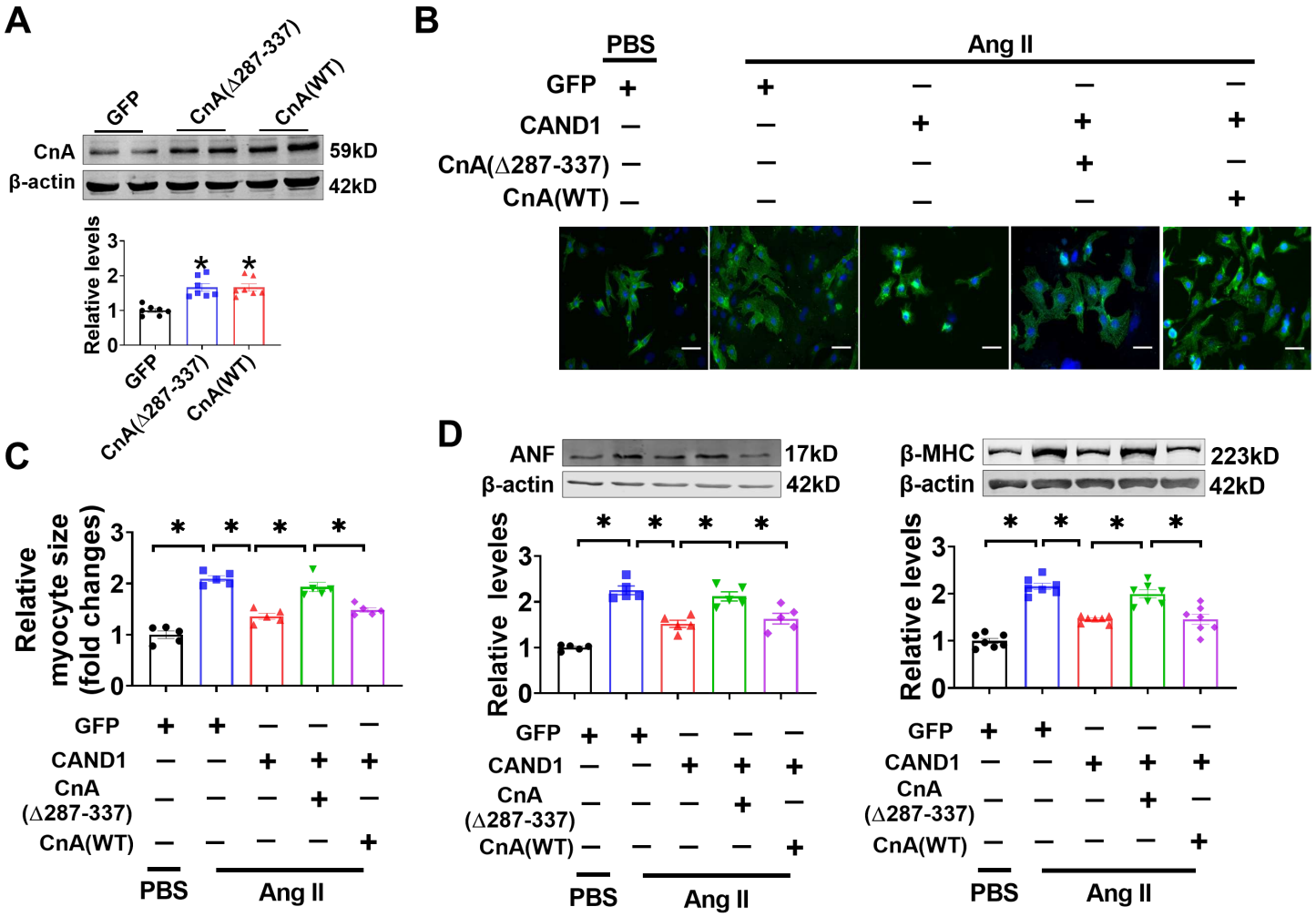

Figure 6

Truncated calcineurin (CnAΔ287-337), but not full-length CnA, abrogated the suppressive effects of CAND1 overexpression on Ang II-induced cardiomyocyte hypertrophy. (A) Protein levels of calcineurin (CnA) in NMCMs transfected with GFP, CnA (WT) and CnA Δ 287-337 (n = 7; *P<0.05). (B) Transfection of CnA (WT) and CnAΔ 287-337 differentially affected protective effects of CAND1 on Ang II-induced enlargement of cardiomyocytes, as indicated by representative images of double immunostaining (green

represents α -actinin for cardiomyocytes; blue indicates DAPI for nuclei). (C) Quantification of myocyte surface area plotted from the data shown in (B) (30 cells counted per experiment; n = 5; *P < 0.05). (D) Protein levels of ANF (n = 5; *P < 0.05) and β-MHC (n = 7; *P < 0.05) obtained under indicated experimental conditions.

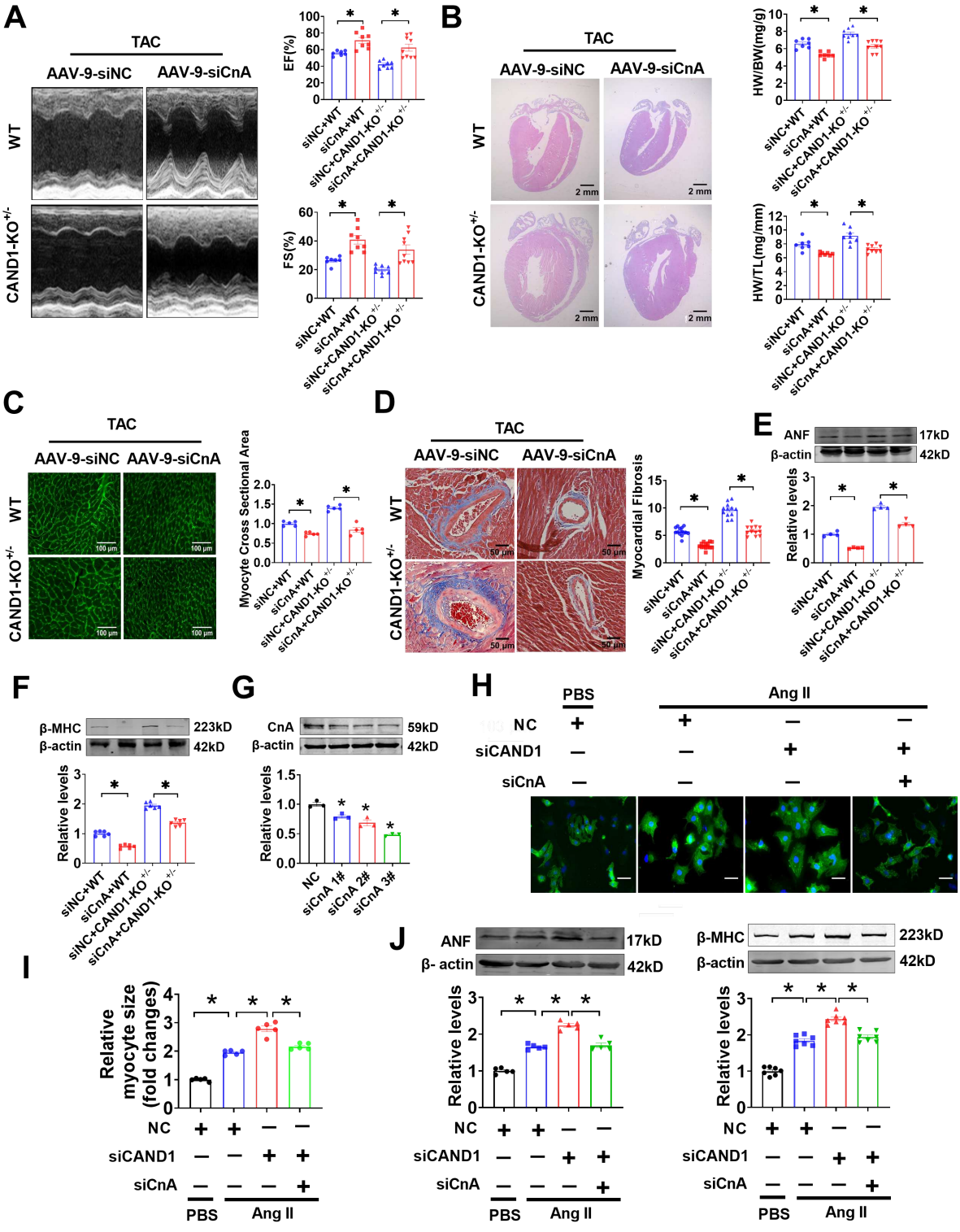

Figure 7

Knockdown of calcineurin improves TAC-induced cardiac dysfunction in CAND1-KO+/- mice. (A) Representative M-mode echocardiography of the hearts and statistical analysis of EF and FS (n = 7-9). (B) Heart size by H&E staining and HW/BW and HW/TL ratios calculated (n = 7-9). (C) Cardiomyocyte size detected by WGA staining and Quantification of the relative myocyte cross-sectional area (200 cells counted per heart) (n = 5) (D) Fibrosis detected by Masson's trichrome staining (n = 5). (E, F) The protein levels of ANF (n = 4) and β-MHC (n = 6). (G) Knockdown efficiency of the siRNAs for CnA in NMCMs (n = 3; *P < 0.05). (H) Representative images of α -actinin and DAPI staining. (I) Quantification of myocyte surface areas (30 cells counted per experiment; n = 5). (J) Protein levels of ANF (n = 5) and β-MHC (n = 7) in NMCMs. Data are presented as mean ± SEM. * P < 0.05 between indicated groups.

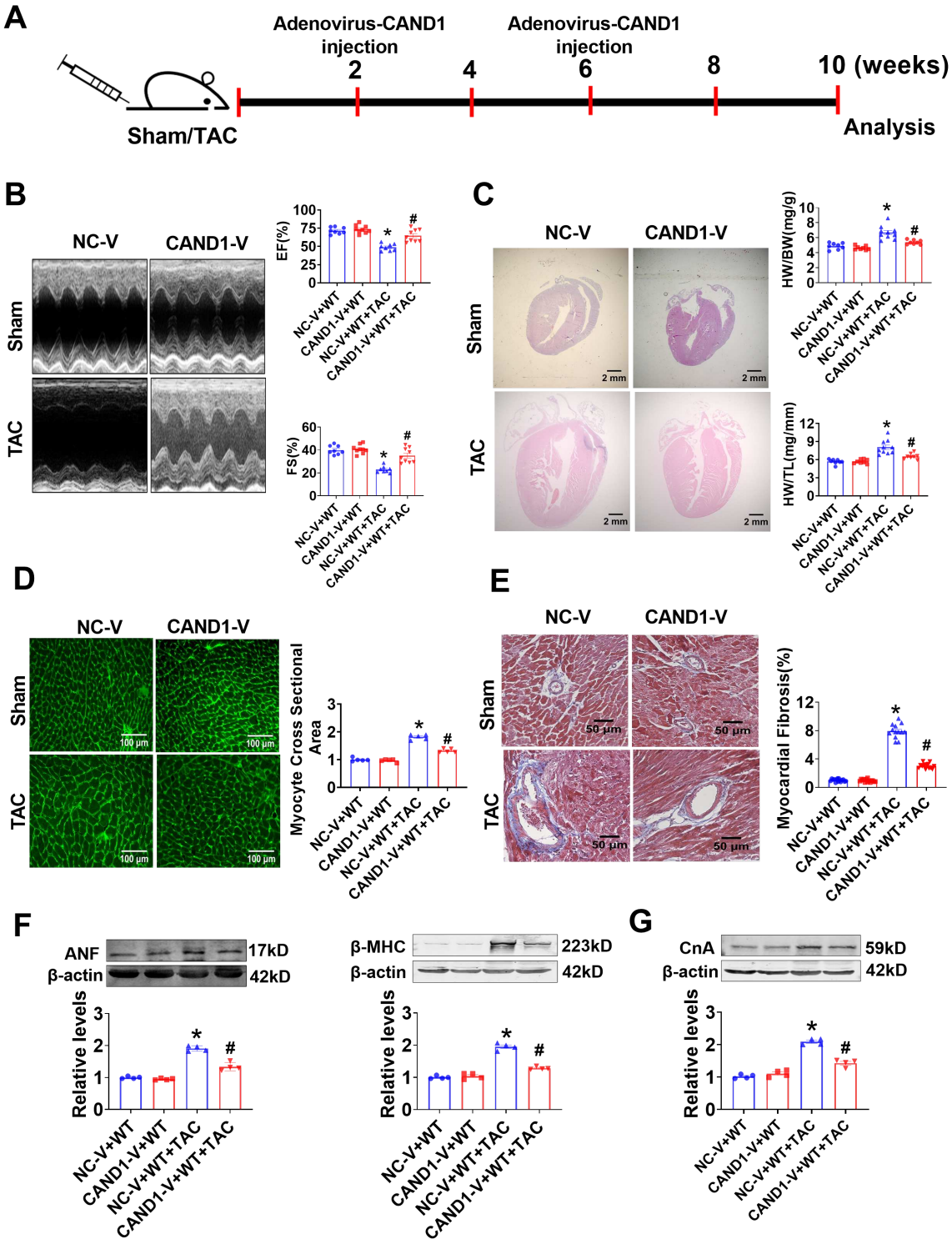

Figure 8

CAND1 overexpression produces anti-hypertrophic effects in TAC model. (A) Representative of the procedures of Ad-CAND1 administration. (B) Representative M-mode echocardiography of the hearts and statistical analysis of EF and FS (n = 8). (C) Heart size detected by H&E staining and HW/BW and HW/TL ratios calculated (n = 8). (D) Cardiomyocyte size detected by WGA staining and quantification of the relative myocyte cross-sectional area (200 cells counted per heart) (n = 5). (E) Cardiac fibrosis detected by

Masson’s trichrome staining and quantification of fibrotic area (n = 5). (F, G) The protein levels of ANF, β-MHC and CnA in the left ventricle (n=4). *P < 0.05, versus WT + V-NC; #P < 0.5, versus WT + TAC + V-NC.

Supplementary Files

This is a list of supplementary files associated with this preprint. Click to download.

- SupplementalMaterialNC.pdf